Journal of Applied Polymer Science

# Thermoplastic Composites of Polyamide-12 Reinforced by Cellulose Nanofibers with Cationic Surface Modification

**Takeshi Semba,[1] Akihiro Ito,[1] Kazuo Kitagawa,[1] Takeshi Nakatani,[2] Hiroyuki Yano,[2] Akihiro Sato[3]**

[1]Department of Organophilic Material Science, Kyoto Municipal Institute of Industrial Technology and Culture, Kyoto, Japan

[2]Research Institute for Sustainable Humanosphere, Kyoto University, Uji, Japan

[3]Chiba Laboratory, New Business Development Division, SEIKO PMC Corporation, Tokyo, Japan

Correspondence to: T. Semba (E-mail: sentake@tc-kyoto.or.jp)

**ABSTRACT:** Cellulose nanofibers (CNFs) have many useful properties, including high strength and low thermal expansion, and are also environmentally friendly, readily renewable, safe, and biodegradable. The focus of this study was the development of lightweight thermoplastic polymer composites with good mechanical properties based on the incorporation of CNFs that have undergone surface pretreatment with a cationic reagent. The polyamide (PA12) was mixed with surface-treated CNFs using a twin screw extruder and the resulting pellets were injection molded. The Izod impact strength without notch of CNF-based composites exceeded that of composites incorporating organophilic montmorillonite (OMMT), a representative nanocomposite material. When the Izod impact test without notch, the impact hammer was stopped by the specimen with incorporation of surface treated CNF. Furthermore, the bending modulus and strength were equal to or greater than that of OMMT composites. The heat distortion temperature was improved as 33°C from neat PA12, and moreover improved as 29°C from OMMT composites. Cationic pretreatment of the CNF surfaces was found to increase the dispersion of the fibers and also to greatly improve the mechanical and thermal properties of the composites. © 2014 Wiley Periodicals, Inc. J. Appl. Polym. Sci. **2014**, *131*, 40920.

**KEYWORDS:** cellulose and other wood products; composites; fibers

Received 2 February 2014; accepted 18 April 2014

**DOI: 10.1002/app.40920**

## INTRODUCTION

In recent years, there has been increasing concern regarding both the availability and the use of petroleum-based resources. These concerns arise for a variety of reasons, including an annual increase in global energy usage of more than 10%, increasing carbon dioxide input into the atmosphere with attendant risks of global warming, serious incidents of environmental pollution associated with oil mining accidents, rapidly increasing crude oil prices owing to political instability in some regions, and finally, the projected depletion of oil stocks over the next several decades. Presently, both the plastics and automotive industries depend on petroleum resources and thus must take responsibility for the associated environmental impacts. Companies in these industries are therefore accelerating the development and adoption of bio-based, environmentally friendly materials. Among the most promising candidates are bio-based polymer composites reinforced by cellulose nanofibers (CNFs). CNFs are readily obtained from renewable resources and, when fabricated at very fine diameter sizes in the order of 4 nm, exhibit diverse and fascinating properties, including strength as much as five times that of steel and the same as that of aramid fibers and low thermal expansion equal to that of quartz glass. CNFs are also environmentally friendly, safe, and biodegradable.[1–7] These outstanding characteristics have attracted much attention and hundreds of research papers dealing with CNFs (including nanocrystal) have been published during the last decade.[8–23] In particular, the automotive industry is interested in finding materials that are lightweight, renewable, and bio-based and yet also exhibit good mechanical properties. The aim of the present study was therefore to investigate the fabrication of lightweight thermoplastic polymer composites incorporating CNFs with good mechanical properties by applying a combination of surface treatment of the CNFs and polymer processing technology. Diverse surface treatments have already been applied to cellulose-based materials during the manufacture of dyed clothes to prevent discoloration, and treatment with positively charged cationic reagents is considered particularly useful[24–26] since the cellulose surface carries a negative charge. Therefore, a number of authors have reported the treatment of nanocellulose with cationic modifiers. The most fundamental investigation was reported, where zeta-potential in solutions at fiber surface was measured in cases of various types

**Table I.** General Properties of PA12 Pellets and Powder

| | DSC analysis | | | | | |
|---|---|---|---|---|---|---|
| | Melting point (°C) | | $\Delta H$ (J/g) | | | |
| | First scan | Second scan | First scan | Second scan | Viscosity number (mg/L) | Particle size ($\mu$m) |
| Pellets | 174.9 | 175.6 | 47.0 | 40.3 | 180 | - |
| Powder | 181.4 | 175.6 | 95.0 | 59.5 | 120 | 10 |

of cationic reagent, this study gave the tip to gain optimum cationized CNFs.[27] As the application study, cationization can induce CNF hydrogels with arbitrary moduli.[28] And combinations of cationized CNFs and layered silicates achieved good water vapor barrier and mechanical properties.[29,30] Thus the positively charge have possibility of functionalization for related nanocellulosic material.

For this reason, cationic reagents have been employed for the surface treatment of CNFs.[31] Treatment with a cationic compound is also predicted to prevent the agglomeration of CNFs during mixing with a polymeric matrix because of the resulting destruction of the hydrogen bond between CNF strands. During the present work, mixtures of the polyamide (PA) PA12 with surface-treated CNFs were compounded using a twin screw extruder and the resulting composite pellets were made into injection moldings to allow for the evaluation of mechanical and thermal properties.

## MATERIAL AND METHODS

### Materials and Preparation

The thermoplastic polymer used as the matrix material in this study was the PA12, in both pellet (commercial name; Daiamid L1940) and powder (commercial name; Vestsint 2159) form, kindly supplied by Daicel-Evonik, Tokyo, Japan. The general properties and physical morphologies of the PA12 materials are shown in Table I and Figure 1, respectively. The PA12 powder had an average particle size of 10 $\mu$m. The PA12 pellets and powder both had equivalent melting points during the second differential scanning calorimeter (DSC) scan (DSC8500; PerkinElmer, Waltham, MA) but the powder exhibited a higher degree of crystallinity during the first and second scans at 10°/min of temperature rising rate in nitrogen atmosphere. The viscosity number from catalog of the pellets was higher than that of the powder owing to a higher molecular weight and/or more branching in the pelletized polymer. In general, because of its high polarity, PA shows good compatibility with many types of

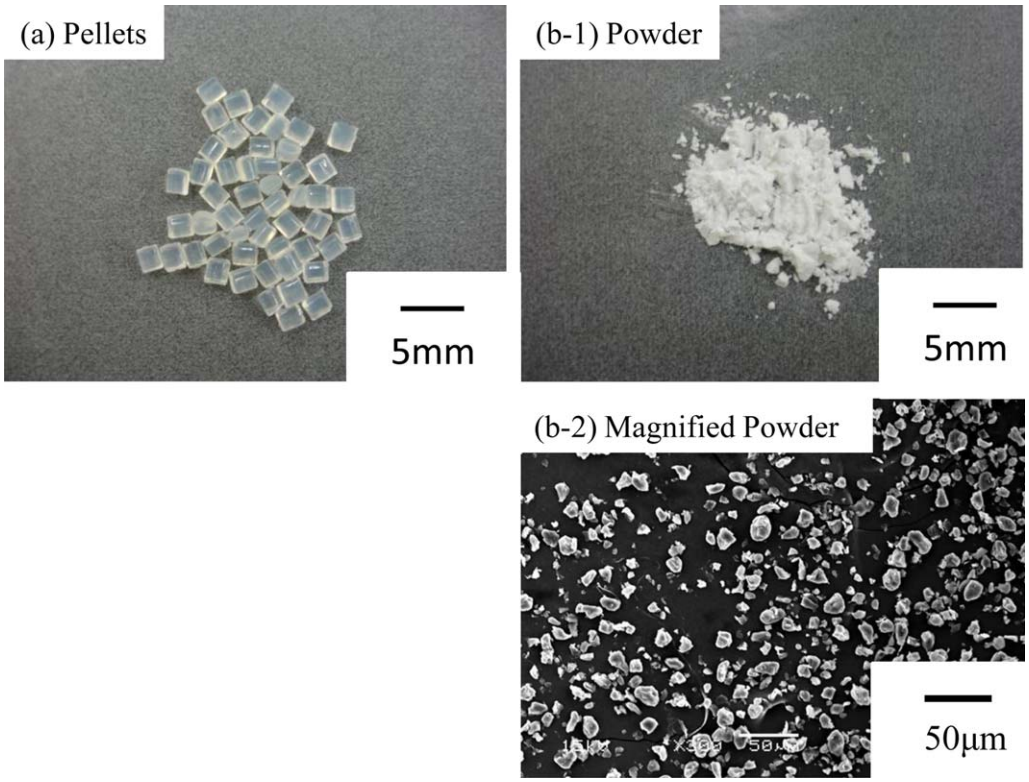


**Figure 1.** Magnified images of PA12 samples used in this study. [Color figure can be viewed in the online issue, which is available at wileyonlinelibrary.com.]

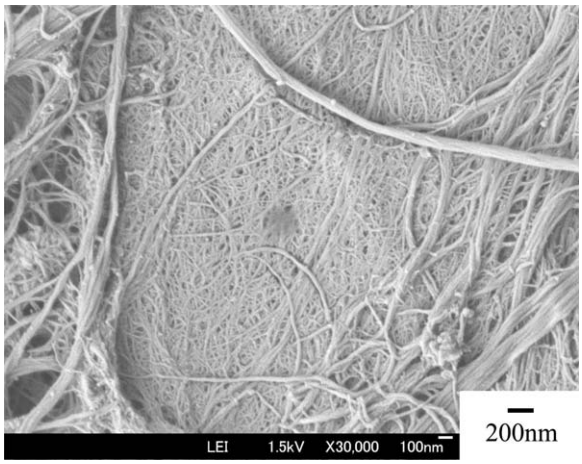


**Figure 2.** Morphology of freeze-dried CNFs.

fillers based on fine-ground or as-synthesized nano-sized minerals. As such, it is reasonable to investigate combinations of CNFs and PA to assess the feasibility of thermoplastic polymer composites incorporating CNFs. The use of PA12 for this purpose presents some advantages because its melting point and processing temperature are significantly lower than those of PA6 and PA66, thus avoiding the high processing temperatures that often cause thermal degradation and lower the performance of cellulose-based materials.

CNF material was supplied from Daicel Chemical Industries, Osaka, Japan. The morphology of the freeze-dried CNFs is shown in Figure 2, in which fine, fibrillated structures can be seen, ranging from a few dozen nanometers to several micrometers in size. The presence of fine structures such as these typically leads to agglomeration when mixing the material with a polymer and so surface pretreatment of the filler is often useful to minimize the agglomeration.

The surface treatment compound applied to the CNFs, kindly supplied by the Senka Corporation, Osaka, Japan, carries a strong positive charge. The basic molecular structure of this compound consists of a backbone of repeating cationic quaternary ammonium units with attached reactive epichlorohydrin groups as shown in Figure 3. The molecular weight of the compound is approximately thirty thousands.

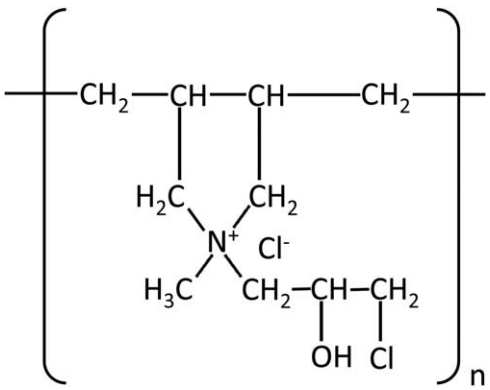


**Figure 3.** Diagram of molecular structure of surface treatment compound.

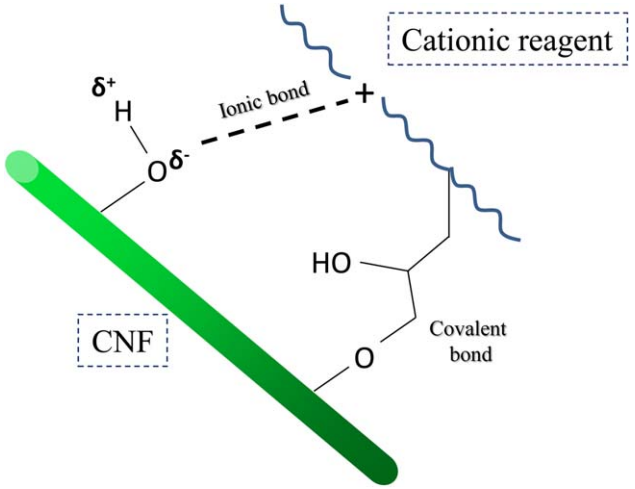


**Figure 4.** Diagram showing bonding between cellulose nanofibers and the cationic reagent. [Color figure can be viewed in the online issue, which is available at wileyonlinelibrary.com.]

The reaction bath composition were CNF of 1.6 wt %, cationic surface treatment compound of 0.5 wt %, sodium hydride of 2.4 wt %, and distilled water of 95.5 wt %, and the reaction was carried out under stirring at 40 °C for 1 h. Subsequently, the cationized fiber was washed in distilled water.

A diagram showing the bonding mechanisms between a CNF and the cationic reagent is provided as Figure 4. The positive charge of the reagent attracts and holds the CNF, allowing the epichlorohydrin groups to efficiently react with the hydroxyl groups of the cellulose to form covalent bonds. Images of filtered CNF cakes (undried and therefore including water) both before and after treatment with the cationic reagent are shown in Figure 5 and it is evident that the general appearance of the material is changed by the treatment. The untreated CNF materials aggregate even in water, whereas the treated CNFs immediately swell when placed in water, indicating the hydrogen bonds between CNF strands are weakened by blocking of the hydroxyl groups, the electrostatic repulsive effect of the cations, and steric hindrance resulting from reactions with the bulky cationic molecules.

In this study, two types of treated CNFs were prepared to compound with the PA12 matrix. The first type of CNF material was thoroughly washed with water following pretreatment with the cationic reagent. The second type was also treated but not washed, and thus contained some residual unreacted cationic reagent on the CNFs. The concentration of reacted cationic reagent contained in the both treated CNF material was estimated at approximately 10 wt % based on elemental analysis by means of total nitrogen analyzer (TN110; Mitsubishi Chemical Analytech, Yokkaichi, Japan). Untreated CNF material was also used for comparison purposes.

During processing, equal weights of PA12 powder and CNFs were mixed together in water, stirred, and then filtered. The addition of PA12 powder to the CNFs in this manner was intended to prevent agglomeration of the CNFs. The resulting 50 wt % CNF and 50 wt % PA12 mixtures were dried and

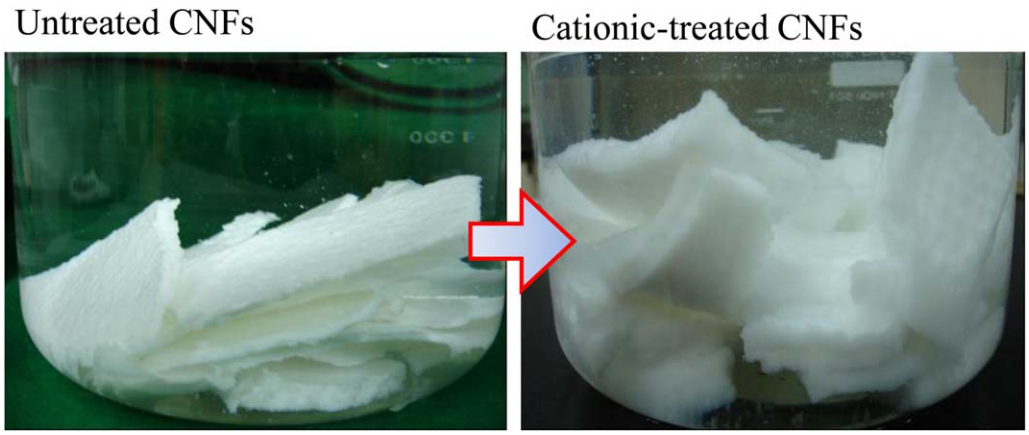


**Figure 5.** Filtered CNF cake before and after cationic treatment. [Color figure can be viewed in the online issue, which is available at wileyonlinelibrary.com.]

ground to powder and subsequently compounded with PA12 pellets.

### Compounding and Fabrication of Specimens

As noted above, CNFs with and without surface pretreatment were first combined with PA12 powder and then were compounded with PA12 pellets by means of a twin screw extruder (screw diameter = 15 mm, screw length/diameter = 45, ZSK 60, Technovel, Osaka, Japan), so as to dilute the cellulose content. Compounding conditions consisted of a throughout cylinder and die temperatures of 190°C and 250 rpm screw revolution. The compounding retention time of materials in the extruder was approximately 180 s. The final composition of the product was PA12 pellets/PA12 powder/CNF = 90/5/5 by weight. Prior to dilution by the addition of PA12 pellets, dilution by PA12 powder was attempted, however, this approach resulted in severe agglomeration of the CNFs in the PA12 matrix. This agglomeration is believed to have occurred because the shear stress generated by the extruder could not be transmitted to the CNFs in the molten PA12 powder because of the low viscosity of the mixture. As a result, the use of PA12 pellets rather than powder was necessary, because this produced a mixture with higher viscosity.

A summary of the various sample specimens that were produced is given in Table II. Sample PA12-P consisted solely of PA12 pellets, PA12-PP was a blend of 5 wt % PA12 powder and 95 wt % pellets, while NT-CNF, C-CNF, and NWC-CNF designate samples made with untreated CNFs, pretreated, washed CNFs, and pretreated, unwashed CNFs. PA12 combined with organophilic montmorillonite (OMMT) was an ideal material for comparison purposes because many groups have reported the merits of PA/OMMT nanocomposites, such as excellent mechanical and thermal properties, resulting from the compatibility of PA with the highly polar OMMT. For this reason, a composite made using OMMT treated with stearyl-dimethyl-benzyl-ammonium-chloride as one of quaternary ammonium salt was used as a comparison material. The OMMT was kindly supplied by the Hojun, Annaka, Japan.

Molded specimens of the compounded materials were produced using a throughout cylinder temperature of 190°C and a cavity temperature of 35°C by means of an injection molding machine

**Table II.** List of Sample Specimens

| | | Material and content (wt %) | | | | | |
|---|---|---|---|---|---|---|---|
| Number | Abbreviated designation | PA12 pellets | PA12 powder | Untreated CNF | Cationic CNF | Unwashed cationic CNF | OMMT |
| 1 | PA12-P | 100 | 0 | 0 | 0 | 0 | 0 |
| 2 | PA12-PP | 95 | 5 | 0 | 0 | 0 | 0 |
| 3 | NT-CNF composite | 90 | 5 | 5 | 0 | 0 | 0 |
| 4 | C-CNF composite | 90 | 5 | 0 | 5 | 0 | 0 |
| 5 | NWC-CNF composites | 90 | 5 | 0 | 0 | 5 | 0 |
| 6 | OMMT composites | 90 | 5 | 0 | 0 | 0 | 5 |

1. PA12-P: Solely PA12 pellets.
2. PA12-PP: PA12pellets/PA12powder = 95/5 (wt %).
3. NT-CNF composites: PA12 pellets/PA12 powder/Untreated CNF = 90/5/5.
4. C-CNF composites: PA12 pellets/PA12 powder/Cationic CNF = 90/5/5.
5. NWC-CNF composites: PA12 pellets/PA12 powder/Unwashed cationic CNF = 90/5/5.
6. OMMT composites: PA12 pellets/PA12 powder/OMMT = 90/5/5.

(NPX-7; Nissei Plastic Industrial, Hanisina, Japan). The moldings time of a cycle was approximately 50 s. Bar-shaped specimens either 4 or 1 mm thick were fabricated for bending tests, the Izod impact test, and measurements of dynamic mechanical properties.

### Dynamic Mechanical Properties

Various tests were performed to assess the potential of CNF-based composites. Dynamic mechanical analysis (DMA) (ARES; TA Instruments, Newcastle, DE) was used because it yields useful information on the interfacial bonding and extent of dispersion of the filler. Dynamic temperature ramp tests were also carried out, using rectangular samples 1 mm thick produced by the injection molding process. Measurements were performed at temperatures ranging from −140 to 200°C, applying a temperature ramp of 3°C/min, 0.1% strain, and a frequency of 6.28 rad/s. The testing mode was torsion rectangular.

### X-ray Computed Tomography

X-ray computed tomography (X-ray CT) is rapidly progressing as an analytical tool and is currently applied not only in medicine but also in various engineering disciplines because it can provide precise three-dimensional (3D) images of internal structures. The resolution of the X-ray CT apparatus (SKY Scan 1172: Bruker-micro CT, Kontich, Belgium) used in this study was 700 nm. Each injection-molded specimen was scanned and 3D images were constructed for the purposes of evaluating the dispersive states of the cellulose fibers. The resolution of 700 nm is insufficient to allow a detailed evaluation of the nanocomposite materials, but the 3D images do offer useful information about agglomeration and aggregation of cellulose fibers in the PA12/CNF composites.

### Bending and Izod Impact Tests

Bending tests of bar-type 4-mm-thick specimens were carried out using a universal testing machine (Autograph AG-5000E; Shimadzu, Kyoto, Japan) at a rate of 10 mm/min and with a 64-mm span length at room temperature. Two types of Izod impact tests were performed on bar-type injection-molded specimens. One test was the normal Izod impact test using a 2.75 J hammer (2.75 J-N) in which the crack propagated from the tip of the notch following striking of the notch side. The second was a reverse Izod impact test using a 5.5-J hammer (5.5 J-R) in which the crack propagated from the opposite side of the notch following striking of the opposite side. The former method evaluates the impact strength, taking into account notch sensitivity, while the latter method evaluates the strength of specimens without the presence of a crack. The fracture surfaces produced by these tests were coated with gold–palladium alloy and studied with a field emission scanning electron microscope (FE-SEM) (JSM6700; JEOL, Tokyo, Japan). The accelerating voltage while observations of fiber and fracture aspect were 1.5 and 5 kV. The lower detector in the evacuated vessel of FE-SEM was employed in this observation to gain sharp observation images.

### Heat Distortion Temperature Tests

Bar-type 4-mm-thick specimens were also used for heat distortion temperature (HDT) tests by three point bending test at span of 64 mm. The HDT values were measured when the distortion displacement of samples reached 0.34 mm when applying a load of either 0.45 or 1.8 MPa and a heating rate of 2°C/min.

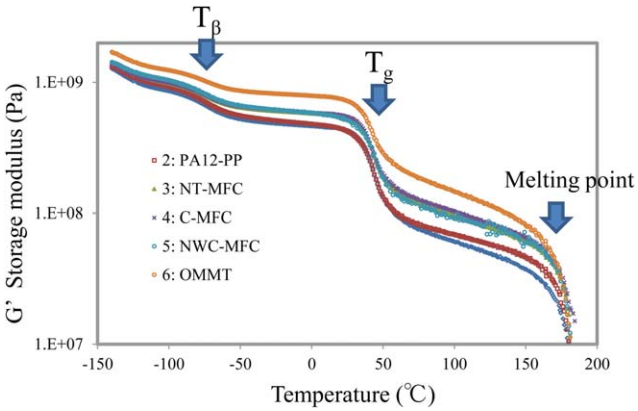


**Figure 6.** (a) Storage modulus curves through whole measured temperature area obtained from DMA. 2. PA12-PP: PA12pellets/PA12powder = 95/5 (wt %); 3. NT-CNF composites: PA12 pellets/PA12 powder/Untreated CNF = 90/5/5; 4. C-CNF composites: PA12 pellets/PA12 powder/Cationic CNF = 90/5/5; 5. NWC-CNF composites: PA12 pellets/PA12 powder/Unwashed cationic CNF = 90/5/5; 6. OMMT composites: PA12 pellets/PA12 powder/OMMT = 90/5/5. (b) Storage modulus curves obtained from DMA. 2. PA12-PP: PA12pellets/PA12powder = 95/5 (wt %); 3. NT-CNF composites: PA12 pellets/PA12 powder/Untreated CNF = 90/5/5; 4. C-CNF composites: PA12 pellets/PA12 powder/Cationic CNF = 90/5/5; 5. NWC-CNF composites: PA12 pellets/PA12 powder/Unwashed cationic CNF = 90/5/5; 6. OMMT composites: PA12 pellets/PA12 powder/OMMT = 90/5/5. (c) Tan $\delta$ curves obtained from DMA. 2. PA12-PP: PA12pellets/PA12powder = 95/5 (wt %); 3. NT-CNF composites: PA12 pellets/PA12 powder/Untreated CNF = 90/5/5; 4. C-CNF composites: PA12 pellets/PA12 powder/Cationic CNF = 90/5/5; 5. NWC-CNF composites: PA12 pellets/PA12 powder/Unwashed cationic CNF = 90/5/5; 6. OMMT composites: PA12 pellets/PA12 powder/OMMT = 90/5/5. [Color figure can be viewed in the online issue, which is available at wileyonlinelibrary.com.]

## RESULTS AND DISCUSSION

### Dynamic Mechanical Properties

The storage modulus ($G$) curves obtained from DMA of sample specimens exhibit three distinct drops at −100, 40, and 160°C, corresponding to the $T_\beta$ ($\beta$ transition temperature), $T_g$ (glass transition temperature), and $T_m$ (melting point) of the PA12 matrix, respectively as shown in Figure 6(a). Three corresponding peaks are also present at these same transition temperatures in the tan $\delta$ plots.

Magnified $G$ plots over the range of 0–100°C are depicted in Figure 6(b) with the OMMT composite data also included to allow comparison. The OMMT material has the highest $G$ value of all the materials tested, which results from its rigidity and also most likely the highly dispersed state of the montmorillonite. The CNF-based composites are intermediate between the OMMT composite and the pure PA12-PP matrix and thus incorporation of CNFs obviously impacts the $G$ value of the material. The cationic pretreatment of the CNFs combined with subsequent washing (the C-CNF composites) further enhances the modulus above 45°C compared with the NT-CNF and NWC-CNF materials. It is possible that the residual cationic

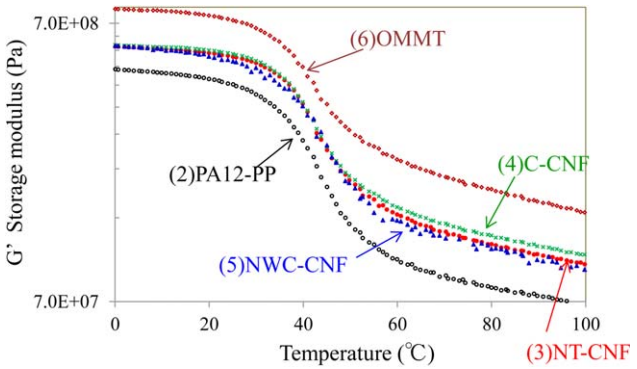


**Figure 7.** X-ray CT images showing internal dispersion states of composites. 2. PA12-PP: PA12pellets/PA12powder = 95/5 (wt %); 3. NT-CNF composites: PA12 pellets/PA12 powder/Untreated CNF = 90/5/5; 4. C-CNF composites: PA12 pellets/PA12 powder/Cationic CNF = 90/5/5; 5. NWC-CNF composites: PA12 pellets/PA12 powder/Unwashed cationic CNF = 90/5/5; 6. OMMT composites: PA12 pellets/PA12 powder/OMMT = 90/5/5. [Color figure can be viewed in the online issue, which is available at wileyonlinelibrary.com.]

reagent in the unwashed NWC-CNF composite acts as a plasticizer and thus affects the modulus.

The tan $\delta$ plots [Figure 6(c)] show the constraint of molecular motion in the PA12 matrix resulting from the incorporation of cationized CNFs, because the peaks of the composites incorporating the pretreated CNFs with and without washing (C-CNF and NWC-CNF) are lower than those of the PA12-PP matrix and the NT-CNF composite. This result is evidence that the dispersion of the CNFs and/or the compatibility between the CNFs and matrix has been improved.

### Three-Dimensional Imaging by Means of X-ray Computed Tomography

Figure 7 shows the internal dispersive state of the CNF-reinforced composites via 3D images obtained from X-ray CT. The lengthwise and crosswise dimensions of the areas shown are 500 $\mu$m and crystalline materials can be seen as bright islets against a dark background. Ideally, a specimen will appear completely dark in the image because this indicates very fine filler dispersion such that the cellulose fibers cannot be detected.

A uniform dark background (with some bright spots of unknown origin) is evident in both the PA12-PP and OMMT composite images. The apparent highly dispersed state of the OMMT composite, representing an ideal nanocomposite structure, is in accordance with the results of the DMA analysis. Conversely, there are many agglomerated cellulose clusters in all of the CNF-reinforced composites. The largest agglomerations in the NT-CNF, C-CNF, and NWC-CNF composites are approximately 100 μm, several tens and a few hundred micrometers in size, respectively. Thus, dispersion of the CNFs varies significantly depending on the pretreatment of the fibers; cationic pretreatment of the cellulose appears to improve dispersion, although unwashed pretreated cellulose negatively affects the dispersive state.

### Bending Tests

Figure 8 provides the stress–strain curves resulting from bending tests. The ductility of the PA12 matrix was maintained in all composites despite the incorporation of rigid fillers, indicating that the fillers used in this study have some degree of compatibility with the PA12 matrix. The NT-CNF and OMMT composites show similar behavior, even though the dispersive state of the NT-CNF composite observed in the X-ray CT image was not as good as that of the OMMT material. These results would imply that the large aspect ratio and network structure of the CNFs enhances the mechanical properties of the NT-CNF composite.

The composites made with pretreated CNFs with and without washing (C-MFC and NWC-MFC) show the greatest improvement in mechanical properties, resulting from the large aspect ratio of the fibers and also most likely good interfacial bonding between the fibers and the matrix. This improved interfacial affinity is evidently sufficient to cancel out any loss in performance brought about by the large agglomerations seen in the X-ray images of the NWC-MFC composite. The inclusion of cationic group destroyed the hydrogen bonds between CNF strands. As a result, reactive hydroxyl groups were exposed on the CNF surface, which could establish new hydrogen bonds with PA12 and improve interfacial adhesion. This types of new hydrogen bond is beneficial for the melt compounding of the CNFs with PA12 as reported by recent literature about the cellulose microcrystalline and poly(vinyl alcohol) composites.[23] In other literature, PA6 nanocomposites filled with cellulose whiskers coated with PA6 was studied. It is a simple and reasonable attempts that exhibited improvements of interfacial adhesion and resulted in heat tolerance properties.[13]

The mechanical properties of all specimens are summarized in Table III, including bending and Izod impact tests. The results obtained for the bending modulus are in good agreement with the DMA results shown in Figure 6(a,b), in which the bending modulus of the OMMT material was the highest of all. In contrast, the strength of the OMMT is similar to that of the NT-MFC and lower than the values obtained for the C-MFC and

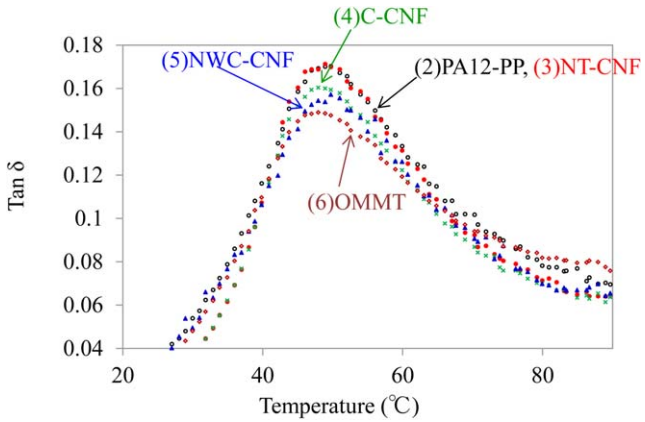


**Figure 8.** Stress–strain curves resulting from bending tests. 2. PA12-PP: PA12pellets/PA12powder = 95/5 (wt %); 3. NT-CNF composites: PA12 pellets/PA12 powder/Untreated CNF = 90/5/5; 4. C-CNF composites: PA12 pellets/PA12 powder/Cationic CNF = 90/5/5; 5. NWC-CNF composites: PA12 pellets/PA12 powder/Unwashed cationic CNF = 90/5/5; 6. OMMT composites: PA12 pellets/PA12 powder/OMMT = 90/5/5. [Color figure can be viewed in the online issue, which is available at wileyonlinelibrary.com.]

**Table III.** Summary of Bending and Izod Impact Test Results

| | | Bending test | | | | Izod impact strength | | | |
|---|---|---|---|---|---|---|---|---|---|
| | | Modulus | | Strength | | 2.75J-N | | 5.5J-R | |
| Number | Abbreviated designation | Value (MPa) | Standard deviation | Value (MPa) | Standard deviation | Value (kJ/m$^2$) | Standard deviation | Value (kJ/m$^2$) | Standard deviation |
| 1 | PA12-P | 1250 | 6.54 | 50.5 | 0.332 | 6.02 | 0.171 | NB | - |
| 2 | PA12-PP | 1160 | 6.84 | 49.8 | 0.534 | 4.29 | 0.154 | NB | - |
| 3 | NT-CNF composite | 1520 | 6.91 | 58.8 | 0.183 | 4.57 | 0.061 | 62.1 | 2.12 |
| 4 | C-CNF composite | 1590 | 4.53 | 61.3 | 0.176 | 4.24 | 0.137 | NB | - |
| 5 | NWC-CNF composites | 1560 | 2.22 | 61.5 | 0.137 | 4.40 | 0.158 | 72.8 | 6.60 |
| 6 | OMMT composites | 1620 | 13.2 | 58.6 | 0.341 | 7.82 | 0.854 | 49.5 | 2.42 |

1. PA12-P: Solely PA12 pellets.
2. PA12-PP: PA12pellets/PA12powder = 95/5 (wt %).
3. NT-CNF composites: PA12 pellets/PA12 powder/Untreated CNF = 90/5/5.
4. C-CNF composites: PA12 pellets/PA12 powder/Cationic CNF = 90/5/5.
5. NWC-CNF composites: PA12 pellets/PA12 powder/Unwashed cationic CNF = 90/5/5.
6. OMMT composites: PA12 pellets/PA12 powder/OMMT = 90/5/5.

NWC-MFC composites. All bending property values were stable and enough to watch significant difference of samples by standard deviation.

### Izod Impact Strength and Fractographic Study

Typical results obtained from the Izod impact test are shown in Table III. All Izod property values were also stable and enough to watch significant difference of samples by standard deviation. In the case of the 2.75 J-N Izod impact test, the OMMT composite, acting as a representative nanocomposite material, exhibited the highest Izod impact strength, surpassing even the unfilled PA12-P and PA12-PP. The composites incorporating CNFs with and without cationic treatment had lower values than the PA12-P, but maintained the same strength level as the pure PA12-PP matrix.

The use of cationic pretreatment with washing (C-CNF) significantly increased the results of the 5.5 J-R Izod impact test. All

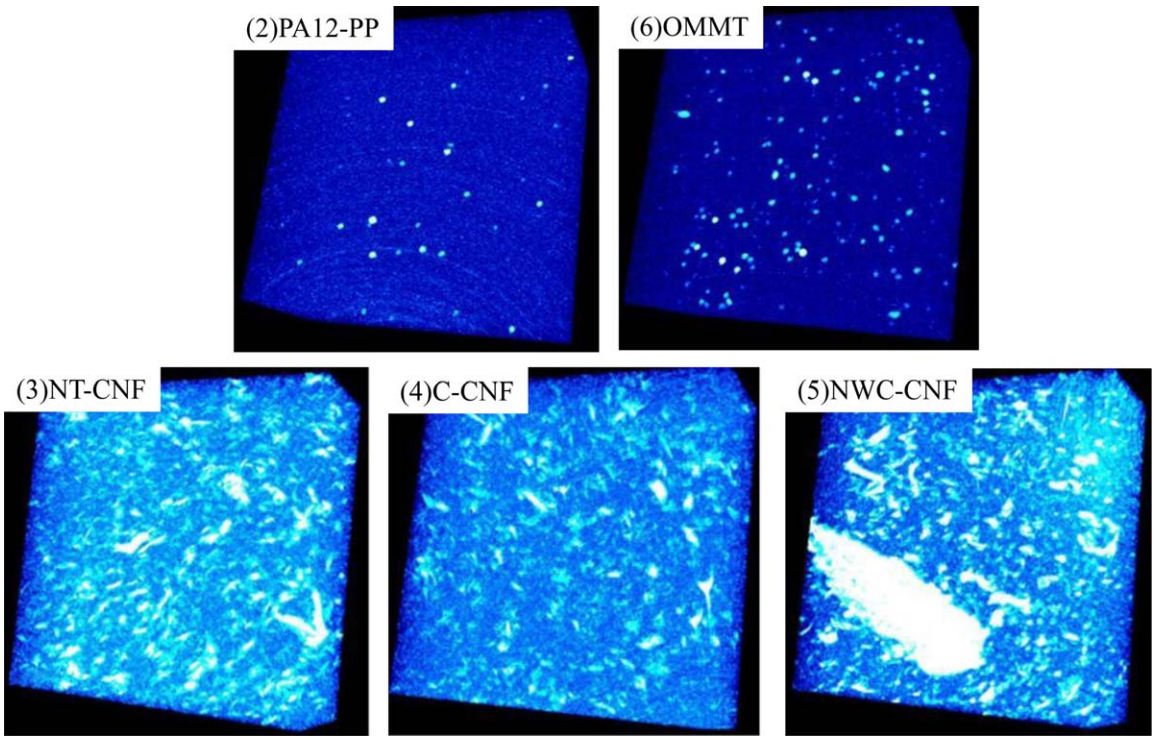


**Figure 9.** Typical fracture surfaces of CNF and OMMT composites. 3. NT-CNF composites: PA12 pellets/PA12 powder/Untreated CNF = 90/5/5; 4. C-CNF composites: PA12 pellets/PA12 powder/Cationic CNF = 90/5/5; 5. NWC-CNF composites: PA12 pellets/PA12 powder/Unwashed cationic CNF = 90/5/5; 6. OMMT composites: PA12 pellets/PA12 powder/OMMT = 90/5/5. [Color figure can be viewed in the online issue, which is available at wileyonlinelibrary.com.]

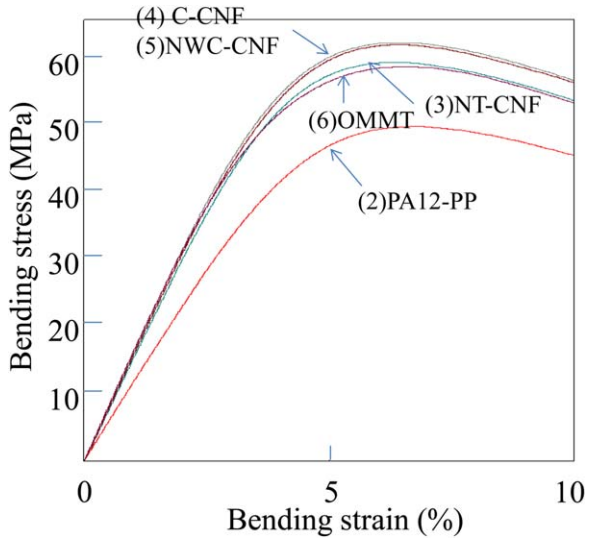


**Figure 10.** (a) HDT curves under 1.8 MPa loading. 2. PA12-PP: PA12pellets/PA12powder = 95/5 (wt %); 3. NT-CNF composites: PA12 pellets/PA12 powder/Untreated CNF = 90/5/5; 4. C-CNF composites: PA12 pellets/PA12 powder/Cationic CNF = 90/5/5; 5. NWC-CNF composites: PA12 pellets/PA12 powder/Unwashed cationic CNF = 90/5/5; 6. OMMT composites: PA12 pellets/PA12 powder/OMMT = 90/5/5. (b) HDT curves under 0.45 MPa loading. 2. PA12-PP: PA12pellets/PA12powder = 95/5 (wt %); 3. NT-CNF composites: PA12 pellets/PA12 powder/Untreated CNF = 90/5/5; 4. C-CNF composites: PA12 pellets/PA12 powder/Cationic CNF = 90/5/5; 5. NWC-CNF composites: PA12 pellets/PA12 powder/Unwashed cationic CNF = 90/5/5; 6. OMMT composites: PA12 pellets/PA12 powder/OMMT = 90/5/5. [Color figure can be viewed in the online issue, which is available at wileyonlinelibrary.com.]

composites except the C-CNF material exhibited complete breaks at the fracture sites following the 5.5 J-R test, while both neat PA12 specimens showed significant distortion owing to their low modulus and strength. The C-CNF composite, however, evidently possesses high impact strength, modulus, and strength and stopped the 5.5-J hammer with only minimal distortion. This is a very promising result with regard to the application of this material as a high-performance composite. In summary, the mechanical properties of the C-CNF composite are equal to or greater than those of the OMMT material and also exhibit high-impact strength.

Typical fracture surfaces at or near the crack initiation areas following the 2.75 J-N test are shown in Figure 9. The distribution of cellulose fibers in the NT-CNF composite was coarser than in the C-CNF and NWC-CNF composites, however, the agglomerated fibers evident in the X-ray CT image are not observed in the fracture surface, probably because they are buried in the PA12 matrix. The fracture surface of the PA12 matrix looks different between the NT-CNF, C-CNF, and NWC-CNF composites; the first two exhibit "muddy" fracture surfaces, whereas the latter surface is more angular. It is believed that residual unreacted cationic reagent around CNFs in the NWC-CNF sample is responsible for this sharpened fracture surface.

### Heat Distortion Temperature Test

Figure 10(a) shows the HDT curves obtained under 1.8 MPa loading. The OMMT- and CNF-reinforced composites show definite improvement over the pure PA12 matrix, such that the points at which deflection occurs are different in materials with and without reinforcements. The slope of the PA12-PP curve is nearly linear with a steep pitch beginning just after the onset of the test and has a final HDT value of 42°C as shown in Table IV. On the contrary, the composites all show improved heat tolerance and low-pitched slopes, especially the C-CNF composite, which has the maximum HDT value of 62.5°C.

Figure 10(b) shows the results of the HDT test under 0.45 MPa loading, where it can be seen in more detail that HDT behavior is affected by surface treatment of the fibers, because the differences are expanded due to the low loading. The HDT curves under 0.45 MPa loading may be classified into two types based on the transition of the deflection displacement. The deflection displacements of the PA12-PP and OMMT composites gradually increase with increasing temperature from 30 to 100°C, then rapidly climb to the maximum displacement of 0.34 mm. The HDT values of these two samples were 107 and 111°C, respectively, as indicated in Table IV. The CNF reinforced composites, however, (NT-CNF, C-CNF, and NWC-CNF) show a different trend between 30 and 100°C; the deflection displacements are constant or decrease over this range and the final HDT values

**Table IV.** Summary of HDT Test Results

| Number | Abbreviated designation | HDT (°C) 1.8 MPa | HDT (°C) 0.45 MPa |
|---|---|---|---|
| 1 | PA12-P | 41.3 | 104 |
| 2 | PA12-PP | 42.0 | 107 |
| 3 | NT-CNF composite | 51.3 | 126 |
| 4 | C-CNF composite | 62.5 | 140 |
| 5 | NWC-CNF composites | 55.7 | 133 |
| 6 | OMMT composites | 51.7 | 111 |

1. PA12-P: Solely PA12 pellets.
2. PA12-PP: PA12pellets/PA12powder = 95/5 (wt %).
3. NT-CNF composites: PA12 pellets/PA12 powder/Untreated CNF = 90/5/5.
4. C-CNF composites: PA12 pellets/PA12 powder/Cationic CNF = 90/5/5.
5. NWC-CNF composites: PA12 pellets/PA12 powder/Unwashed cationic CNF = 90/5/5.
6. OMMT composites: PA12 pellets/PA12 powder/OMMT = 90/5/5.

are higher than that of the OMMT composite. The highest HDT value was obtained with the C-CNF composite at 140°C. These data demonstrate that the inclusion of only 5 wt % of cationic pretreated CNFs dramatically improved the heat resistance of the PA12 composites owing to the high aspect ratio of the CNFs, as well as improvements in the interfacial adhesion between the CNFs and the PA12.

## CONCLUSIONS

The results of this study illustrate the potential of composite materials incorporating CNFs. The destruction of the hydrogen bonds between CNF strands, and steric hindrance resulting from reactions with the bulky cationic reagent used to pretreat the CNFs improved both the distribution of the fibers and the interfacial adhesion between the CNFs and the PA12. These improvements resulted in enhanced bending and Izod impact strength properties as well as better thermal resistance. These useful properties of CNF composites are derived from the excellent distribution and unprecedented high aspect ratio of the fibers. We believe that, having demonstrated excellent mechanical and thermal properties, bio-based and ultra-lightweight CNF-based composites are well suited to numerous applications, especially as structural materials, for example, automotive parts, housing of various household electrical appliances, in situations requiring weight reduction in glass- or carbon fiber-reinforced materials.

## REFERENCES


1. Jonoobi, M.; Harun, J.; Mathew, A. P.; Oksman, K. *Compos. Sci. Technol.* **2010**, *70*, 1742.
2. Page, D. H.; El-Hosseiny, F. *J. Pulp Paper Sci.* **1983**, *84*, 99.
3. Nishino, T.; Arimoto, N. *Biomacromolecules* **2007**, *8*, 2712.
4. Henriksson, M.; Berglund, L. A.; Isaksson, P.; Lindström, T.; Nishino, T. *Biomacromolecules* **2008**, *9*, 1579.
5. Abe, K.; Iwamoto, S.; Yano, H. *Biomacromolecules* **2007**, *8*, 3276.
6. Abe, K.; Yano, H. *Cellulose* **2009**, *16*, 1017.
7. Nakagaito, A. N.; Iwamoto, S.; Yano, H. *Appl. Phys. A* **2005**, *80*, 93.
8. Eichhorn, S. J.; Dufresne, A.; Aranguren, M.; Marcovich, N. E.; Capadona, J. R.; Rowan, S. J.; Weder, C.; Thielemans, W.; Roman, M.; Renneckar, S.; Gindl, W.; Veigel, S.; Keckes, J.; Yano, H.; Abe, K.; Nogi, M.; Nakagaito, A. N.; Mangalam, A.; Simonsen, J.; Benight, A. S.; Bismarck, A.; Berglund, L. A.; Peijs, T. *J. Mater. Sci.* **2010**, *45*, 1.
9. Moon, R. J.; Martini, A.; Nairn, J.; Simonsen, J.; Youngblood, *J. Chem. Soc. Rev.* **2011**, *40*, 3941.
10. Nakagaito, A. N.; Nogi, M.;, Yano, H. *MRS Bull.* **2010**, *35*, 214.
11. Abbott, A. P.; Bell, T. J.; Handa, S.; Stoddart, B. *Green Chem.* **2006**, *8*, 784.
12. Mihranyan, N. G.; Razaq, A.; Lindström, T.; Nyholm, L.; Strømme, M. *J. Phys. Chem. B* **2010**, *114*, 4178.
13. Corrêa, A. C.; Teixeira, E. M.; Carmona, V. .; Teodoro, K. B. R.; Ribeiro, C.; Mattoso, L. H. C.; Marconcini, J. M. *Cellulose* **2014**, *21*, 311.
14. Suzuki, K.; Okumura, H.; Kitagawa, K.; Sato, S.; Nakagaito, A. N.; Yano, H. *Cellulose* **2013**, *20*, 1, 201.
15. Kamphunthong W.; Hornsby, P.; Sirisinha, K. *J. Appl. Polym. Sci.* **2012**, *125*, 1642.
16. Fortunati, E.; Puglia, D.; Monti, M.; Santulli, C.; Maniruzzaman, M.; Kenny, J. M. *J. Appl. Polym. Sci.* **2013**, *128*, 3220.
17. Xiang, C.; Taylor, A. G.; Hinestroza, J. P.; Frey, M. W. *J. Appl. Polym. Sci.* **2013**, *127*, 79.
18. John, M. J.; Anandjiwala, R.; Oksman, K.; Mathew, A. P. *J. Appl. Polym. Sci.* **2013**, *127*, 274.
19. Dahman, Y.; Oktem, T. *J. Appl. Polym. Sci.* **2012**, *126*, E188.
20. Kose, R.; Kondo, T. *J. Appl. Polym. Sci.* **2013**, *128*, 1200.
21. Martínez-Sanz, M.; Lopez-Rubio, A.; Lagaron, J. M.; *J. Appl. Polym. Sci.* **2013**, *128*, 2666.
22. Wu, J. H.; Kuo, M. C.; Chen, C. W.; Chen, C. W.; Kuan, P. H.; Wang, J. H.; Jhang, S. Y. *J. Appl. Polym. Sci.* **2013**, *129*, 3007.
23. X, Sun; C, Lu; Y, Liu; W, Zhang; X. Zhang. *Carbohydr. Polym.* **2014**, *101*, 642.
24. Hashem, M.; Hauser, P.; Smith, B. *Text. Res. J.* **2003**, *73*, 1017.
25. Khalil-Abad, M. S.; Yazdanshenas, M. E.; Nateghi, M. R. *Cellulose* **2009**, *16*, 1147.
26. Zghida, H.; Baouab, M. H. V.; Gauthier, R. *J. Appl. Polym. Sci.* **2003**, *87*, 1660.
27. Alila, S.; Boufi, S.; Belgacem, M. N.; Beneventi, D. *Langmuir* **2005**, *21*, 8106.
28. Dong, H.; Snyder, J. F.; Williams, K. S.; Andzelm, J. W. *Biomacromolecules* **2013**, *14*, 3338.
29. Ho, T. T.; Zimmermann, T.; Ohr, S.; Caseri, W. R. *ACS Appl. Mater. Interfaces* **2012**, *26*, 4, 4832.
30. Ho, T. T.; Zimmermann, T.; Hauert, R.; Caseri, W. R. *Cellulose* **2011**, *18*, 1391.
31. Semba, T.; Itou, A.; Kitagawa, K.; Nakatani, T.; Yano, H. Proceeding of Asian Workshop on Polymer Processing 2012, Published by The Japan Society of Polymer Processing. Tokyo Japan, 245.